Title
Modeling the Ionic Strength Effect on Diffusion in Clay. The DR-A Experiment at Mont Terri

Journal
ACS Earth and Space Chemistry, 3(3)

ISSN
2472-3452

Authors
Soler, Josep M
Steefel, Carl I
Gimmi, Thomas
et al.

Publication Date
2019-03-21

DOI
10.1021/acsearthspacechem.8b00192

Peer reviewed

Modeling the Ionic Strength Effect on Diffusion in Clay. The DR-A Experiment at Mont Terri

Josep M. Soler,[*,†] Carl I. Steefel,[‡] Thomas Gimmi,[§,∥] Olivier X. Leupin,[⊥] and Veerle Cloet[⊥,#]

[†] IDAEA-CSIC, Jordi Girona 18-26, 08034 Barcelona, Catalonia, Spain [‡] Lawrence Berkeley National Laboratory, Berkeley, California 94720, United States [§] Paul Scherrer Institut, CH-5232 Villigen PSI, Switzerland [∥] University of Bern, CH-3012 Bern, Switzerland [⊥]NAGRA, CH-5430 Wettingen, Switzerland

* E-mail: josep.soler@idaea. csic.es.

Present Address # (V.C.) Arcadis, CH-8952 Schlieren, Switzerland.

Abstract

Solute diffusion in compacted clays depends on ionic strength through its control on the thickness of the electrical double layer (EDL) on the charged clay surfaces. In the DR-A field experiment (Mont Terri, Switzerland), synthetic porewater was circulated through a borehole for 189 days, leading to the out-diffusion of a variety of tracers into the Opalinus Clay. The borehole solution was then replaced with a higher-salinity solution for an additional 540 days, leading to the diffusion of Cs^+, Ca^{2+}, Mg^{2+}, and Sr^{2+} back into the borehole and to an increase in the out-diffusion of anions (I^-, Br^-) and ^3H. The experimental results were interpreted using the CrunchClay code, which includes a mean electrostatic potential model for the EDL. The EDL corresponds to a second continuum in addition to bulk electrically neutral porewater. Species-specific diffusion (Nernst–Planck equation) occurs through both domains. A 1D radial model considered a single pore diffusion coefficient ($D_p = 10^{-9}$ m^2/s) for cations and ^3H in the bulk porosity, and a smaller D_p (3×10^{-10} m^2/s) for anions. D_p values in the EDL were smaller (10^{-11} m^2/s), except for Cs^+ and K^+ (5×10^{-10} and 2×10^{-10} m^2/s, respectively). The model reproduced well the experimental results and showed the capability to consider temporal changes in geochemical conditions affecting the transport and retention of potentially important radionuclide contaminants (e.g., $^{137}Cs^+$, $^{90}Sr^{2+}$, $^{129}I^-$) in underground geological nuclear waste repositories. Coupled multicomponent diffusion together with the electrostatic properties of the charged surfaces are essential in the development of predictive models for ion transport in clays.

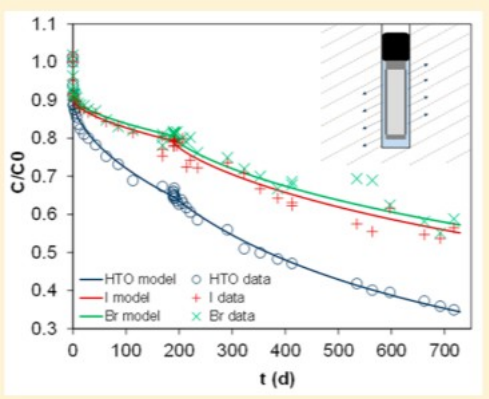

KEYWORDS: Clay, diffusion, sorption, porosity, anion exclusion, EDL

1. Introduction

Argillaceous formations are considered as suitable host rocks for the geological disposal of radioactive waste in a number of countries (e.g., France, Belgium, Canada, Switzerland). These rocks are characterized by very low permeabilities with solute transport controlled by diffusion, and high clay contents favoring sorption and retention of cations. Diffusion in these compact clay-rich rocks shows a dependency on ionic strength, which is linked to the properties of the electrical double layers (EDL) bordering charged clay mineral surfaces. A mechanistic understanding of this dependence is necessary for any model predictions of the evolution of this type of clay-rich systems.

The Mont Terri rock laboratory (St. Ursanne, Switzerland) is an international multidisciplinary project running since 1996 and it provides an opportunity to study radionuclide migration in the Opalinus Clay Formation (Jurassic). The DR-A in situ diffusion experiment was performed between November 2011 and November 2013 in the DR-A niche of the rock laboratory. The rock formation was the shaly facies of the Opalinus Clay (OPA).

Several diffusion experiments had already been performed at Mont Terri (DI, FM-C, DI-A1, DI-B, DI-A2, DR).(1−19) In those experiments, synthetic porewater at equilibrium with the rock and containing tracers was continuously circulated through a packed-off borehole interval and the decrease in tracer concentrations in the liquid phase was monitored. Subsequently, a volume of rock surrounding the borehole was overcored and the tracer profiles in the rock were analyzed. The results showed the value of the experimental setup and the importance of processes such as anion exclusion and sorption of cations.

After those first experiments, the DR-A test was designed to provide insight on solute transport coupled to relevant processes such as anion exclusion and competing sorption by cation exchange. The first stage of the DR-A test consisted of a conventional diffusion experiment using a synthetic version of the OPA porewater, including several tracers. After 189 days, the solution in

the borehole was replaced with a higher-salinity solution (0.50 M NaCl + 0.56 M KCl). The effect of the change in ionic strength on solute transport was to be investigated.

The effect of the formation of EDLs on ion concentration and transport in porous materials with charged solid surfaces has been the subject of intense research in the last two decades.(20−24) The case of the clays, and especially smectite interlayers in compacted bentonite (overlapping EDLs), has received special attention due to its relevance in the geologic disposal of radioactive waste.(25−31)

The calculations presented here correspond to the modeling of the experimental results from the DR-A experiment (evolution of solute concentrations in the circulation system and profiles in the rock) using the CrunchClay software, a variant of CrunchFlow that includes an explicit treatment of the EDL based on a mean electrostatic model.(32) These calculations are based on a new modeling approach that had not been used in previous experiments at Mont Terri (those experiments had only involved synthetic OPA porewater). A similar approach for the inclusion of the EDL in reactive transport codes has already been described by Appelo and Wersin. (10) A simplified implementation has also been recently reported by Gimmi and Alt-Epping.(33)

2. Overview of the Experiment

The experiment was performed in the shaly facies of Opalinus Clay at Mont Terri. The closed circulation system (reservoir tank, lines, borehole interval) contained 10.243 L of solution. The reservoir tank was pressurized with argon to avoid pressure gradients between the system and the rock, and it was placed on a weighing scale to detect any possible inflows or outflows of water. A magnetic drive gear pump was used for circulation. Flow rate was 25 mL/min. Figure 1 shows the experimental setup (tracer circulation interval). The solution was circulated through a small gap (0.5 mm) between the central tube and the filter. There was another gap (3 mm thick) between the filter and the borehole wall. Circulation of the tracers was started on November seventh, 2011, and lasted until November fifth, 2013.

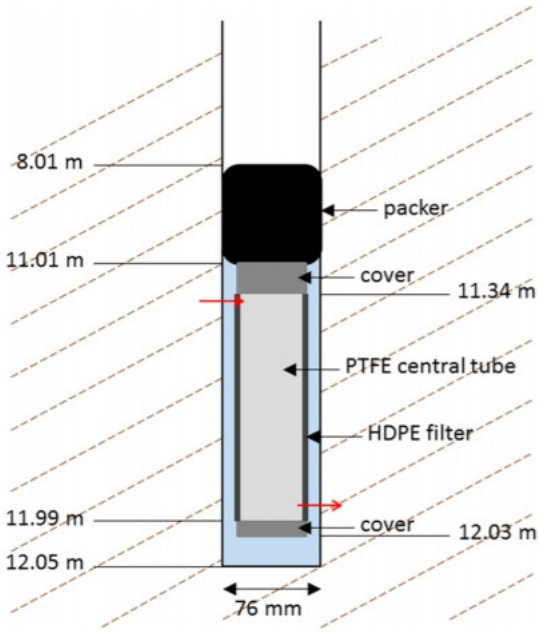

Figure 1. Schematics of the circulation interval. Solution was circulated through a small gap (0.5 mm) between the central tube and the filter. Dashed lines indicate bedding. Red arrows show the positions of the inlet and outlet ports. The light blue area corresponds to the open part of the borehole interval.

Synthetic porewater (NaCl-dominated, ionic strength 0.36 molal) containing tracers was circulated through the borehole for 189 days. The tracers were HTO (^{3}H; water tracer), I^- and Br^- (anionic tracers subject to anion exclusion), Cs^+ and $^{85}Sr^{2+}$ (cations sorbing by cation exchange), and $^{60}Co^{2+}$ and Eu^{3+} (cations presumably sorbing strongly by surface complexation). After this period the synthetic porewater was replaced with a higher-salinity solution (0.50 M NaCl + 0.56 M KCl; more $^{85}Sr^{2+}$ added) for an additional 540 days. Replacement of the solution was performed by switching circulation from the initial reservoir tank to a second tank containing the high-salinity solution. Switching to the new solution led to diffusion of Cs^+, Ca^{2+}, Mg^{2+} and Sr^{2+} back into the borehole resulting from desorption and to an increase in the out-diffusion of anions (I^-, Br^-) and also of HTO. This increase in out-diffusion is hypothesized to be related to the increase in ionic strength of the water and its effect on the thickness of the EDL on the clay surfaces. At the end of the experiment the borehole equipment was removed, the borehole was filled with resin, and an overcore was drilled with a larger diameter to obtain rock samples for further analysis.

3. Model Description

Since transport in OPA is dominated by diffusion along the bedding planes (preferential fast pathways for diffusion)(34) and transport distances are short compared to the length of the injection interval, a one-dimensional (1D) approach with symmetry with respect to the borehole axis was deemed

sufficient to model the results. However, the borehole in DR-A was drilled vertically at an angle of about 60° with respect to bedding (dip of bedding is about 30°). In principle, this geometry does not allow for a direct application of a 1D radially symmetric model around the borehole axis. However, by modifying the borehole radius and capacity, a 1D implementation was achieved.

The 1D radial diffusion-sorption calculations considering the formation of an EDL bordering the negatively charged clay surfaces and species-specific diffusion based on the Nernst–Planck equation have been performed using the CrunchClay reactive transport code.(32,35)

The diffusion equation in saturated porous media represented as a single continuum takes the form

 (1)

where J_i is the diffusive flux of species i and ${}^{tot}C_i$ is the total concentration of the species (moles per bulk volume, mol/m^3) given by

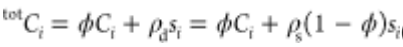 (2)

and C_i is the aqueous concentration of the species (moles per fluid volume, mol/m^3), ϕ is porosity, ρ_d is the bulk dry density of the rock (kg/m^3), s_i is the concentration of sorbed species (moles per mass of solid, mol/kg), and ρ_s is the solid density of the rock (2740 kg/m^3).

Tournassat and Steefel(35) reviewed the basics of the application of the Nernst–Planck equation to the diffuse layer bordering charged surfaces in reactive transport codes. This approach is used in CrunchClay, a dual continuum version of CrunchFlow(32) that allows for the explicit calculation of accumulation and transport within bulk and EDL (also called diffuse layer) porosities. The EDL porosity is treated with a mean electrostatic model, which can be thought of as an averaging of the Poisson–Boltzmann equation. (36) The fundamental assumption of the model is that rapid equilibrium between the diffuse layer and bulk water compositions is achieved within a representative elementary volume (grid cell). With this assumption, it is possible to describe the diffusive flux within the diffuse layer with an equation having the same form as the Nernst–Planck equation for the bulk porosity, given here in one dimension

 (3)

where J_i is the diffusive flux of the species i, which has an effective diffusion coefficient $D_{e,i}$, a charge z_i, a bulk concentration ${}^{b}c_i$, and an activity coefficient ${}^{b}\gamma_i$. The superscript b/EDL indicates that the parameter must be defined for the bulk water or the diffuse layer water, depending on the

diffusive flux of interest. The term A_i corresponds to an accumulation/depletion factor of cations and anions in the diffuse layer compared to bulk water. $A_i = 1$ in the bulk water porosity and $A_i = e^{-z_i F \psi_{EDL}/RT}$ in the EDL porosity, ψ_{EDL} is the mean electrical potential in the EDL porosity, F is the Faraday constant, R is the gas constant, and T is the temperature.

When applied to a system where diffuse layer water and bulk water are present, eq 1 in one dimension becomes

 (4)

where ${}^{b}J_i$ and ${}^{EDL}J_i$ are fluxes in bulk and diffuse layer water as defined in eq 3. Expanding eq 3 for bulk and diffuse layer water, we obtain

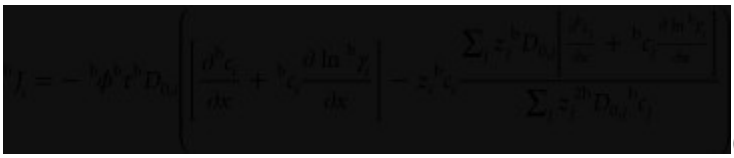 (5)

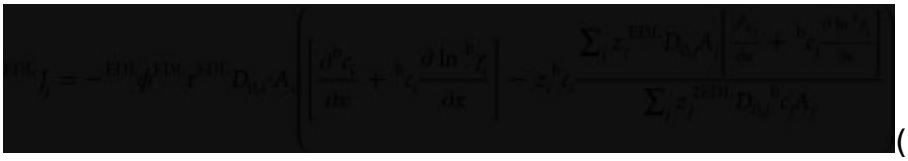 (6)

where $D_{0,i}$ is the self-diffusion coefficient of the species i, and τ is a tortuosity term that is specific to each type of porosity and medium (${}^{b/EDL}D_{e,i} = {}^{b/EDL}\phi\ {}^{b/EDL}\tau\ {}^{b/EDL}D_{0,i}$).

The EDL porosity is dynamically calculated according to

$${}^{EDL}\phi = \text{Area}_{clay}\lambda_{DL}D_L \quad (7)$$

where Area_{clay} is the area of clay (m^2/m^3) and λ_{DL} is the number of Debye lengths (used here as an adjustable model parameter). The Debye length D_L, which provides an approximate measure of the thickness of the EDL, is given by

$$D_L = \frac{\beta_{DL}}{\sqrt{I}} \quad (8)$$

where β_{DL} is a constant (3.0×10^{-10} m $(mol/L)^{1/2}$ at 25 °C) and I is the ionic strength of the bulk solution. In the calculations shown here total porosity ${}^{Tot}\phi$ has been fixed to 0.15. Therefore, the bulk porosity is

$${}^{b}\phi = {}^{Tot}\phi - {}^{EDL}\phi \quad (9)$$

Solute concentrations in the EDL are related to concentrations in the bulk solution through the A_i term (${}^{EDL}C_i = A_i {}^{b}C_i$).

Figure 2 shows a schematic representation of the pore domains in the rock.

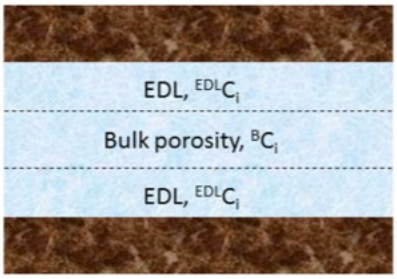

Figure 2. Schematic diagram showing the pore domains in the rock (EDL and bulk porosities) and the associated diffusion coefficients.

In the results presented here, the fitting of the model to the experimental data involved the adjustment of the number of Debye lengths (λ_{DL}), which is used to calculate the EDL porosity (eq 7), and of the pore diffusion coefficients (D_p) for water, cations, and anions in both the EDL and bulk porosities. λ_{DL} and D_p values are constant throughout the calculation in the model. D_e values change due to the changes in ionic strength, which imply changes in bulk and EDL porosities. Total porosity and clay (Illite) properties (volume fraction, specific surface area, surface charge, CEC and cation exchange model) were fixed based on previous studies, as discussed in Section 4. However, a small modification of the cation exchange model was required for a better match of the model to the measured data.

4. Setup, Dimensions, and Model Parameters

Figure 1 shows the experimental setup (tracer circulation interval) and Table1 shows the relevant parameters for the simulations. The solution was circulated through a small gap (0.5 mm) between the central tube and the filter.

Table 1. Parameters for Modeling

length of interval	104 cm
borehole diameter	76 mm
filter, outer diameter	70 mm
filter, inner diameter	62 mm
filter, porosity	45%
gap filter–borehole wall	3 mm
dip of bedding	32.5°

For a correct description of the borehole geometry with respect to the orientation of the bedding planes (preferential planes for diffusion), the model has to take into account that the intersection between borehole and bedding is actually elliptical. The length of this intersection affects the magnitude of the solute fluxes between borehole and rock. However, in the 1D radial model used here the borehole section is by definition circular. An adjusted borehole radius (41.6 mm) was calculated assuming that the outer circumference was equal to the perimeter of the elliptical intersection between bedding plane and borehole. The area of the circle with the newly calculated radius is 1% larger than the area of the ellipse, which is relevant

for the calculation of the volume of the borehole (volume of solution). Therefore, the borehole capacity α_b (volume of solution per volume of borehole interval) was reduced by the same factor (1%). The same correction was applied to filter and gap. As a result, in the model the filter has a thickness of 4.38 mm and a porosity equal to 44.5%. The gap between filter and borehole wall has a porosity of 98.9%. The validity of the implementation was checked by comparing the results from 2D and 1D-radial models (only single tracer transport).

The volume of water in the circulation system (tank, lines, inner gap) was 10.243 L, which translated into a capacity value of the borehole α_b equal to 3.262 (it does not include the filter and gap between filter and borehole wall). Fast diffusion (well-mixed conditions) was assumed for the borehole and filter (possible fluid circulation through the filter). Otherwise, the implementation of measured filter diffusion coefficients (D_e about 10^{-10} m^2/s), resulted in the formation of solute concentration gradients across the filter which prevented a good match between model results and measured data, mainly for sorbing species. For those species (e.g., Cs^+), the measured fast initial drop in concentration in the circulation system (borehole) could not be reproduced due to the slow diffusive transport through the filter.

Synthetic porewater containing tracers was circulated through the borehole for 189 days, after which it was replaced with a higher-salinity solution for an additional 540 days. Tables2 and 3 show the initial solution compositions in the model, which are based on the measurement of solution chemistry during the experiment.

Table 2. Initial Solution Compositions in the First Stage of the Experiment (Total Concentrations in mol/kg_H_2O)[a]

	borehole	rock/filter/gap
T (°C)	18	18
pH	7.6	7.6
Na^+	2.59×10^{-1}	2.59×10^{-1}
K^+	1.64×10^{-3}	1.64×10^{-3}
Mg^{2+}	1.80×10^{-2}	1.80×10^{-2}
Ca^{2+}	1.88×10^{-2}	1.88×10^{-2}
Sr^{2+}	5.10×10^{-4}	5.10×10^{-4}
Cl^-	2.78×10^{-1}	3.00×10^{-1}
SO_4^{2-}	1.37×10^{-2}	1.37×10^{-2}
HCO_3^-	8.18×10^{-3} charge balance	7.25×10^{-3} charge balance
Cs^+	2.069×10^{-4}	2.0×10^{-8}
SiO_2(aq)	6.71×10^{-5} Quartz	6.71×10^{-5} Quartz
Al^{3+}	1.18×10^{-8} Illite	1.18×10^{-8} Illite
I^-	1.09×10^{-2}	1.00×10^{-12}
Br^-	1.09×10^{-2}	7.15×10^{-4}
HTO	1.21×10^{-10}	1.21×10^{-16}

[a]The borehole composition is based on measurements at t = 169 d with pH fixed at 7.6 (laboratory measurement before the start of the experiment) and imposing equilibrium with respect to quartz and Illite. HCO_3^- is calculated by charge balance. Mineral solubilities from the EQ3/6 database included in CrunchFlow.[41]

Table 3. Initial Solution Composition in the Borehole for the Second Stage of the Experiment (t = 189 Days; Total Concentrations in mol/kg H_2O)[a]

	borehole
T (°C)	18
pH	7.6
Na^+	5.00×10^{-1}
K^+	5.60×10^{-1}
Mg^{2+}	1.47×10^{-2}
Ca^{2+}	2.30×10^{-2}
Sr^{2+}	4.54×10^{-4}
Cl^-	1.118 charge balance
SO_4^{2-}	2.37×10^{-4}
HCO_3^-	5.63×10^{-4} equil. atmosphere
Cs^+	6.23×10^{-6}
SiO_2(aq)	5.76×10^{-5} Quartz
Al^{3+}	2.88×10^{-9} Illite
I^-	8.60×10^{-3}
Br^-	8.86×10^{-3}
HTO	7.84×10^{-11}

[a]The borehole composition is based on measurements at t = 189 d with pH fixed at 7.6 and imposing equilibrium with respect to quartz and Illite. HCO_3^- is calculated by equilibrium with atmospheric CO_2 and Cl^- by charge balance. Mineral solubilities from the EQ3/6 database included in CrunchFlow.[41]

Sorption has been modeled using a multisite cation exchange for OPA.(37−39)Table4 shows the parameters of the cation exchange model (Gaines-Thomas convention) used in the calculations. The original log *K* value for K^+–Na^+ exchange on the planar sites (PS-K reaction) had to be changed from −1.1 to −0.4 (weaker affinity of K^+ for the planar sites). Otherwise, the results showed too much sorption of K^+ compared with the measured data. Note that the previous in situ experiments had only involved the use of synthetic OPA porewater (lower ionic strength), and the sorption behavior on the low-affinity planar sites had not really been tested. log *K* for Sr^{2+}–Na^+ exchange was assigned a value of −1.0 by calibration with the measured experimental data. Also, the capacity of the planar sites had to be increased by 20% (from 9.5×10^{-2} to 1.14×10^{-1} eq/kg) for a better model match of the Ca and Mg concentrations in the rock profiles. The total cation exchange capacity (0.1225 eq/kg) is in good agreement with the values of about 0.120 eq/kg reported by Waber et al.(40) for the location of the DR-A experiment within the Opalinus Clay.

Table 4. Exchange Reactions, Selectivity Coefficients (log *K*) and Site Capacities (eq per kg of Solid Rock) for the Multisite Cation Exchange Model (OPA)[a]

	log *K*	Site capacity (eq/kg)
FES-Cs + Na^+ = FES-Na + Cs^+	−7.0	1.05×10^{-4}
FES-K + Na^+ = FES-Na + K^+	−2.4	
II-Cs + Na^+ = II-Na + Cs^+	−3.6	8.4×10^{-3}
II-K + Na^+ = II-Na + K^+	−2.1	
PS-Cs + Na^+ = PS-Na + Cs^+	−1.6	1.14×10^{-1}
PS-K + Na^+ = PS-Na + K^+	−0.4	
PS2-Ca + $2Na^+$ = 2PS-Na + Ca^{2+}	−0.67	
PS2-Mg + $2Na^+$ = 2PS-Na + Mg^{2+}	−0.59	
PS2-Sr + $2Na^+$ = 2PS-Na + Sr^{2+}	−1.0	

[a]FES, II, and PS refer to frayed-edge, type II, and planar sites, respectively.

The total number of solution species in the calculations was 62. Speciation reactions were from the EQ3/6 database included in CrunchFlow.(41) Activities were calculated with an extended Debye–Hückel formulation (b-dot model).

Concerning the EDL parameters in the rock, a surface charge of −0.2 eq/kg for Illite was assumed, which is equivalent to the cation exchange capacity of Illite.(37) The volume fraction and specific surface area of Illite in the rock were fixed to 0.20(26) and 100 m^2/g,(42) respectively. Note that the proved application of the Illite cation exchange model to the Opalinus Clay(37−39) only considers the Illite content of the rock. The same approach was used here, also for the calculation of the EDL properties.

Fitting of the model to the experimental results required the use of 4 Debye lengths ($\lambda_{DL} = 4$). Otherwise it was not possible to obtain enough difference in the transport parameters when changing from OPA porewater to the high

salinity solution (different values in the bulk and EDL porosities). Note also that according to the diffuse double layer model(43) the surface potential actually falls exponentially with distance from the surface, and it is smaller by a factor of 1/e (0.368) at 1 Debye length, and by a factor of 0.018 at 4 Debye lengths (bulk concentrations would be found after about 4 Debye lengths from the charged surface). All this translated into initial bulk and EDL porosities in the rock equal to 0.0397 and 0.1103, respectively. Total porosity was fixed to 0.15, according to the findings in previous laboratory and field experiments.(12,19)

Typical reported anion-accessible porosities of the Opalinus Clay at Mont Terri, assuming total exclusion of anions in the nonaccessible porosity, are about 50% to 60% of the total porosity.(12,17) The 4 Debye lengths that were used in the calculations, together with the total Cl^- concentrations in both the bulk and EDL porosities, translate into an initial anion-accessible porosity in the rock equal to 57% of the total porosity.

It should be mentioned that in the approach used here, cation exchange (Table4) and EDL are uncoupled. On one hand, the model makes use of a well-established multisite nonelectrostatic cation exchange model. Cation exchange does not consider the EDL, and exchange is between the clay surface and the bulk solution. Surface charge used for the calculation of the EDL is independent of the cation exchange capacity in the modeling presented here, although this is not a requirement of the CrunchClay software, which can consider fully coupled surface complexation and surface charge. Note however that the permanent structural charge of Illite may range from −1.9 to −2.8 eq/kg_{Illite},(42) while its cation exchange capacity is approximately 0.2 eq/kg_{Illite}.(37) Therefore, the surface charges corresponding to the cation exchange complex and to the EDL could be both accommodated by the large value of the permanent structural charge. This approach allows (i) the combination of the well-established cation exchange model for cation sorption on the clay with an explicit treatment of the EDL, and (ii) the model reproduction of the measured exchangeable cation contents in the rock, as discussed in Section 5.3.

Effective diffusion coefficients (D_e) in the model were calculated according to (Figure 2, eqs 5 and 6)

$$^{b/EDL}D_{e,i} = {}^{b/EDL}\phi^{b/EDL}\tau^{b/EDL}D_{0,i} \quad (10)$$

The following tortuosity (τ) values were used: 3.07×10^4 (borehole), 2.25×10^4 (filter), 2.02 (gap), 1.0 (rock). The values apply to both bulk and EDL porosity. Since the value of τ in the rock is 1.0, the value of D_0 (constant throughout the calculations) is equivalent to the pore diffusion coefficient D_p ($D_p = D_e/\phi$). D_0 values were adjusted to match model results to experimental data. Large τ-values in borehole and filter allow the implementation of large effective diffusion coefficients (well-mixed conditions). Table5 shows the initial D_e values in the model. Since negligible

surface charge was assigned to the borehole, filter and gap, they do not contain any EDL porosity. As a result, D_e values do not change when the salinity changes. However, D_e values in the rock will change as bulk porosity increases and EDL porosity decreases with increasing salinity (the Debye length changes according to eq 8). The initial net value for HTO (4.08×10^{-11} m^2/s) is consistent with the results of modeling without explicit treatment of the EDL and with previous experimental results.(19) Note also that it was necessary to assign large diffusion coefficients to the Cs^+ and K^+ species in the EDL, consistent with larger net D_e values for strongly sorbing cations.(44) This is interpreted to be the result of fast diffusive transport of these cations in the EDL or within a Stern layer.(20,21,44)

Table 5. Initial Species-Specific D_e Values in the Different Domains of the Calculation[a]

	borehole bulk porosity D_e (m^2/s)	filter bulk porosity D_e (m^2/s)	gap bulk porosity D_e (m_2/s)	rock bulk porosity D_e (D_p) (m^2/s)	rock EDL porosity D_e (D_p) (m^2/s)
cations and neutral species	1×10^{-4}	1×10^{-5}	2×10^{-9}	3.97×10^{-11} (10^{-9})	1.10×10^{-12} (10^{-11})
anions	3×10^{-5}	3×10^{-6}	6×10^{-10}	1.19×10^{-11} (3×10^{-10})	1.10×10^{-12} (10^{-11})
Cs^+	1×10^{-4}	1×10^{-5}	2×10^{-9}	3.97×10^{-11} (10^{-9})	5.52×10^{-11} (5×10^{-10})
K^+	1×10^{-4}	1×10^{-5}	2×10^{-9}	3.97×10^{-11} (10^{-9})	2.21×10^{-11} (2×10^{-10})

[a] D_p values are also indicated for the rock domain. Large D_e values in borehole and filter result in well-mixed conditions for those domains. The differences between cations/neutral species and anions in borehole, filter and gap are a consequence of the different species-specific D_0 values for the bulk porosity used in the model.

Differences in D_p in the rock between bulk and EDL porosities, and also between cations and anions, may be caused by the different geometries of the diffusion pathways near the clay surfaces (EDL) compared to those in the centers of the pores (bulk). Pore throats where EDLs from opposite walls overlap may be the reason for the smaller D_p values for anions in the bulk porosity. Pore throats would have a stronger effect on anions, due to the limited access of anions to the EDL.

5. Results and Discussion

Stage 1 of the DR-A experiment (OPA porewater) lasted 189 days and stage 2 (high-salinity solution) lasted 540 days, totaling 729 days. At the end of stage 2 the borehole equipment was removed and filling of the borehole with resin and chalk gravel was attempted. On the following day it was realized that resin did not fill the borehole completely and that some water was present at the bottom of the borehole. Some of this water could be pumped out of the borehole and resin was injected again. Overcoring and rock sampling was performed on day 735. The modeling presented here only covers the 729 days of the experiment (stages 1 and 2). The last 6-day period is probably responsible for the back-diffusion signals visible in the first 3–4 cm of the tracer profiles in the rock. These back-diffusion transport distances are consistent with a time period of 6 days when estimating diffusion distances with the Einstein equation in 2D ($\langle x \rangle^2 = 4D_p t$). However, this short period of back-diffusion does not affect the profiles further away from the borehole wall.

The reported modeling results do not include $^{85}Sr^{2+}$ (C_0 = 4000 Bq/L = 5.4 × 10^{-14} mol/L), $^{60}Co^{2+}$ (C_0 = 600 Bq/L = 2.4 × 10^{-14} mol/L) and Eu^{3++} (C_0 = 10^{-6} mol/L). Because of its short half-life (64.85 d), no $^{85}Sr^{2+}$ could be detected in the rock profile samples. Also, accurate modeling of $^{85}Sr^{2+}$ would need the explicit incorporation of radioactive decay to $^{85}Rb^{+}$ and its sorption by cation exchange. $^{60}Co^{2+}$ (strongly sorbing by surface complexation) was only detected in some of the measured profiles up to about 1 cm from the borehole wall. It was not possible to measure Eu^{3+} in the rock probably due to sorption onto equipment parts of the borehole circulation system. Experimental results for HTO correspond to activities corrected for decay back to the beginning of the experiment.

5.1. Concentrations in the Circulation System

Major-element concentrations were measured by ion chromatography (IC), inductively coupled plasma-optical emission spectroscopy (ICP-OES), and inductively coupled plasma-mass spectrometry (ICP-MS), as described in Gimmi et al. (in their Supporting Information file),(17) for the previous DR experiment. HTO activities were measured by liquid scintillation counting, as described in Wersin et al.,(12) also for a previous experiment (DI-A2). Errors in the measured concentrations were about ±10% for Cl^- and Na^+, ±3% for HTO and ±5% for all other tracers and solutes.

Figure 3 shows the evolution of solute concentrations in the circulation system. It is noteworthy that out-diffusion of the tracer anions I^- and Br^- from the borehole increased after the replacement of the solution in the borehole (faster drop in concentrations). This also affected HTO, although the effect was less. The model reproduced these trends well. When salinity increases (stage 2), EDL porosity decreases and bulk porosity increases (Figure 4). Because diffusion coefficients in the bulk porosity are larger than in the EDL (Table5), the net diffusion coefficient increases and accelerates out-diffusion. The decrease in concentration for Br^- is slightly slower than for I^- due to the larger background concentration in the rock (7.15 × 10^{-4} mol/L for Br^- compared to virtually no I^-).

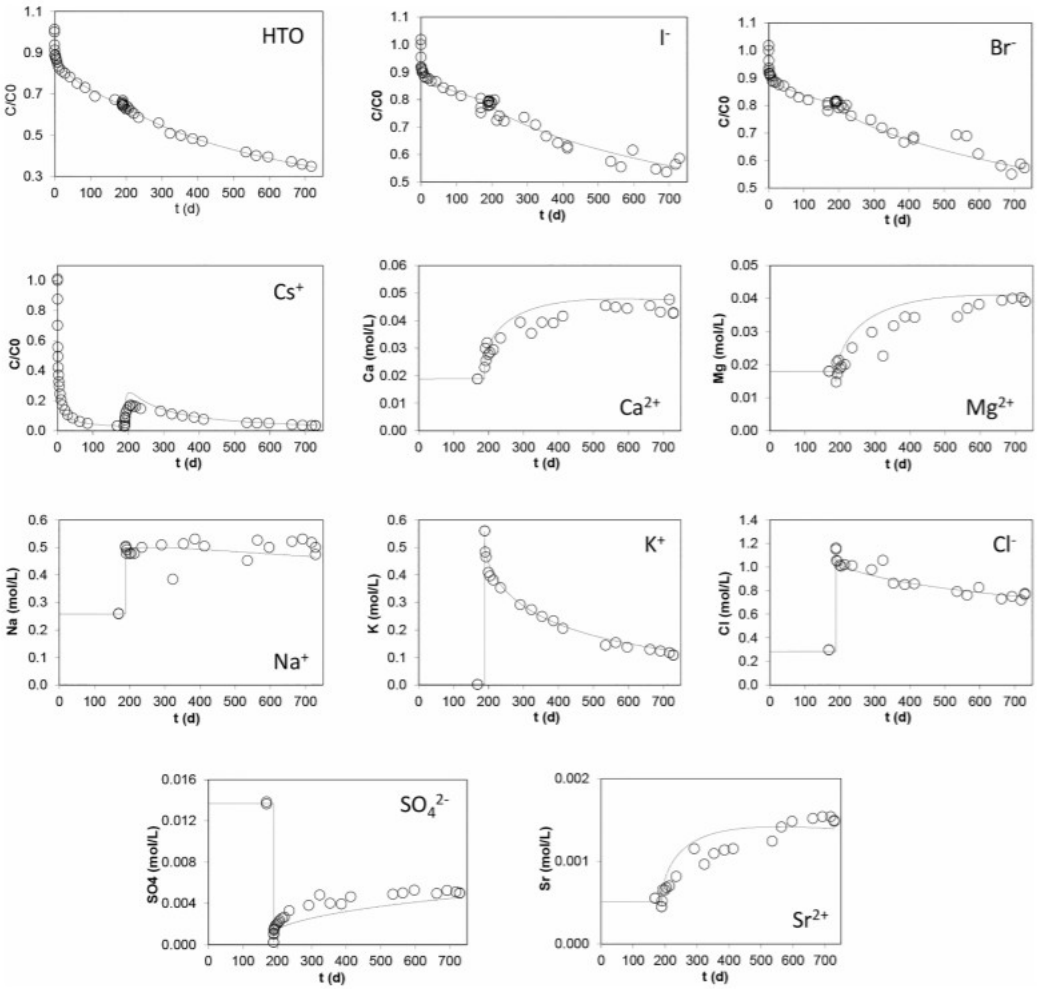

Figure 3. Evolution of solute concentrations (total concentrations or relative concentrations) versus time in the circulation system (borehole). Lines correspond to model results and symbols to measured data.

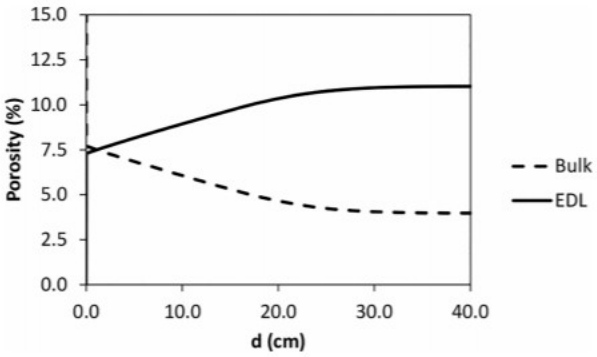

Figure 4. Calculated bulk and EDL porosities versus distance from the borehole wall at t = 729 d (total porosity fixed at 15%). Porosities far from the borehole are equal to the initial porosities. Close to the borehole they have changed due to the advance of the high salinity front.

Cs^+ shows a rapid drop in concentration at early times due to the strong sorption in the rock. However, after replacing the solution in the borehole,

Cs^+ is displaced from the exchange complex by K^+ and partially diffuses back to the borehole, causing a temporary increase in concentration. At about 200 days, shortly after the replacement of the borehole solution, concentration decreases again due to diffusion and sorption into the rock.

Back-diffusion (from rock to borehole) due to desorption is also observed for Ca^{2+}, Mg^{2+}, and Sr^{2+}. The high-salinity solution had Na^+ and K^+ concentrations that were higher than the background concentrations in the rock. K^+ concentration began to decrease after the replacement of the solution in the circulation system due to strong sorption in the rock, which caused displacement of Ca^{2+}, Mg^{2+}, Sr^{2+}, and Na^+ from the exchange complex. A positive concentration gradient (higher concentration in the rock and lower in the borehole) was created for Ca^{2+}, Mg^{2+}, and Sr^{2+} but not for Na^+ due to its high concentration in the borehole.

Regarding Cl^-, the high-salinity solution also had a concentration much higher than the background concentration in the rock. Cl^- concentration began to decrease after the replacement of the solution in the circulation system. SO_4^{2-} concentration started increasing after solution replacement, since the high-salinity solution contained very little SO_4^{2-} compared to the Opalinus Clay porewater. Overall, the simulations reproduced well the changes in concentrations in the circulation system.

5.2. Aqueous Extract Data

Aqueous extracts from rock samples were obtained according to the procedure described in Gimmi et al.(17) Centimetric rock samples of known weight were quickly transferred into an oxygen-free glovebox after overcoring, where they were dried under ambient temperature. Afterward they were subject to grinding in a ring mill outside of the glovebox. Aqueous extracts were prepared in polypropylene tubes from about 30 g of rock material (grain size <63 μm) and about the same mass of degassed, oxygen- and CO_2-free water. After 24 h under continuous shaking, the solutions were filtered within the glovebox (0.45 μm) and the supernatant was used for the chemical analyses. Measurements were performed at the Paul Scherrer Institut (PSI) and at the University of Bern (UB). These aqueous extracts allow the determination of porewater concentrations for nonsorbing tracers and solutes. However, the measured concentrations for sorbing cations may be subject to disturbances.

Figure 5 shows measured and calculated profiles for HTO (Bq per gram of porewater), Cl^-, I^-, and Br^- (mol/L). Note that the calculated HTO concentrations in the bulk and EDL porosities are identical, due to the electrically neutral character of HTO (no effect of surface charge on concentration). For Cl^-, I^-, and Br^-, the experimental data fall between the calculated values for bulk and EDL porosities, as expected.

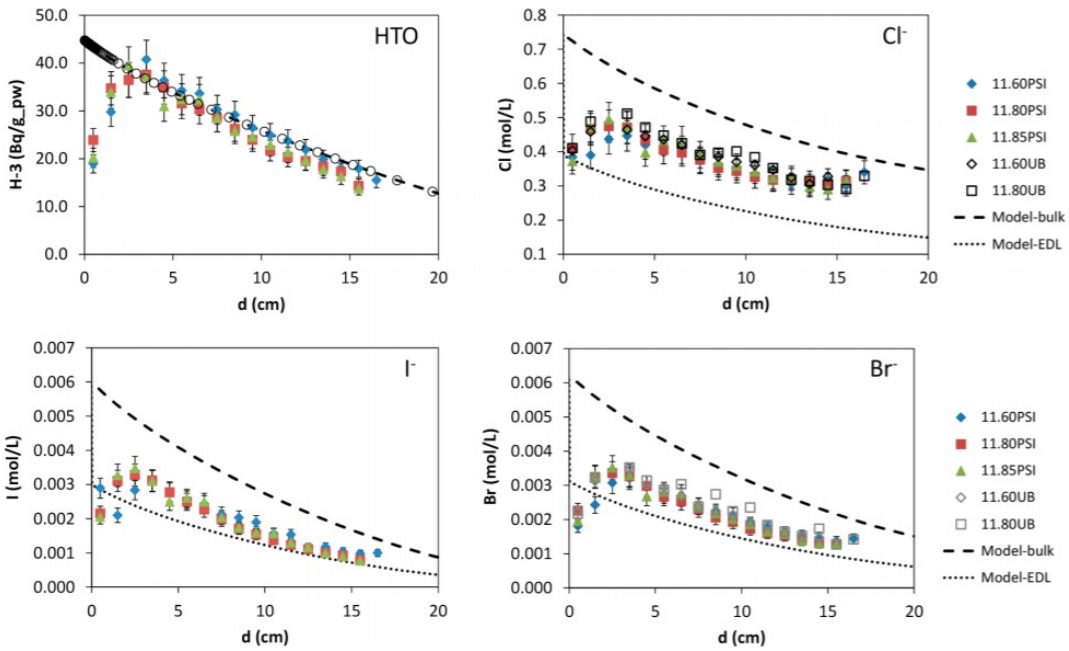

Figure 5. HTO, Cl^-, I^-, and Br^- contents versus distance from the borehole wall. Black dashed lines correspond to the bulk porosity in the model (t = 729 d); black circles (HTO) or dots (Cl^-, I^-, Br^-) correspond to the EDL porosity in the model (t = 729 d); colored and gray symbols correspond to data measured at PSI and/or UB (aqueous extracts) for three different rock profiles. The profiles are identified by the distance (m) along the borehole (see Figure 1). The measured increase in concentration at the outer boundary (furthest from the borehole) is most likely an experimental artifact due to heating during overcoring.

Overall, model results reproduce well the observed solute distributions in the profiles, which reflect diffusion from the borehole to the rock through the two different pore domains (bulk and EDL). As discussed above, the measured lower concentrations in the first 3–4 cm of rock probably reflect back-diffusion to the borehole during the 6 days between partial filling of the borehole with resin and overcoring.

5.3. Ni-Ethylenediamine Extract Data

Figure 6 shows calculated and measured concentrations corresponding to Ni-ethylenediamine extracts performed at the University of Bern. The extraction procedure, which allows the measurement of the amounts of cations sorbed on the cation exchange complex plus the amounts present in the porewater, is based on the method described by Baeyens and Bradbury(45,46) and in Pearson et al.(47) A 0.1 M Ni-ethylenediamine solution prepared with degassed, ultrapure water was used. The wet rock material was immediately immersed into the solution without previous drying. The suspensions prepared on site at a liquid to rock ratio of about 1 were transferred on the same evening to the laboratory in Bern. There, they were shaken for 7 days under ambient conditions. The solutions were prepared such that the equivalents of Ni-ethylenediamine added were about twice the exchange capacity. Separation of liquid and solid occurred by centrifugation followed by filtration (0.45 µm) of the supernatant solution. Cations and Ni in the Ni-ethylenediamine solutions were analyzed by ICP-OES.

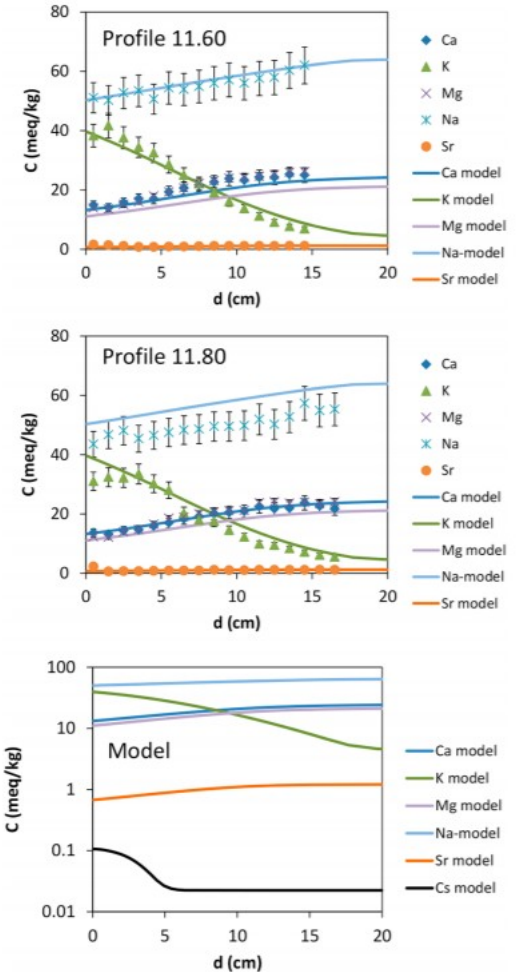

Figure 6. Calculated (lines) and measured (symbols) concentrations ($meq/kg_{wetrock}$) corresponding to the Ni-ethylenediamine extractions performed at Univ. Bern in two rock profiles. The profiles are identified by the distance (m) along the borehole (see Figure 1). The plot at the bottom (only model results) also shows the calculated Cs^+ concentrations.

Experimental data and calculated values are in good agreement. Match between model results and measurements is slightly better in profile 11.60 for Na^+ and in profile 11.80 for Ca^{2+} and Mg^{2+}. Measured porosities ranged between 0.15 and 0.16 in samples from profile 11.80 and between 0.17 and 0.18 in samples from profile 11.60. Figure 6 also shows the calculated Cs^+ concentrations, which were not measured. Note that they are much smaller than those of the other elements.

Again, the cation distribution profiles in the rock reflect diffusion from the borehole to the rock through the two different pore domains plus retention by cation exchange. In the second stage of the experiment K^+ displaces Na^+, Ca^{2+}, Mg^{2+}, Sr^+, and Cs^+ from the exchange complex.

6. Conclusions

Modeling of the DR-A experiment at Mont Terri, involving the study of salinity changes on solute diffusion and retention in the Opalinus Clay, has been performed using the CrunchClay code. The inclusion in the model of (i) the effect of the EDL on diffusion, (ii) multisite cation exchange, (iii) smaller diffusion coefficients in the EDL compared to those in the bulk porosity, and (iv) smaller diffusion coefficients in the bulk porosity for anions compared to those for cations and neutral species, allowed the reproduction of both the changes in concentrations in the borehole and the solute distribution profiles in the rock. The model reproduced well the experimental results and showed the capability to consider temporal changes in geochemical conditions affecting the transport and retention of potentially important radionuclide contaminants (e.g., $^{137}Cs^{+}$, $^{90}Sr^{2+}$, $^{129}I^{-}$) in underground geological nuclear waste repositories. The modeling of the experiment highlights the need to consider coupled multicomponent diffusion (Nernst–Planck equation) together with the electrostatic properties of the charged surfaces in order to develop predictive models for ion transport in clays.

Acknowledgments

Partial financial support was provided by the Mont Terri Project (Switzerland), thanks to the partners of the DR-A experiment (NAGRA, Switzerland; NWMO, Canada; Department of Energy, U.S.A.). C.S. acknowledges funding support from the Director, Office of Science, Basic Energy Sciences, Chemical Sciences, Geosciences, and Biosciences Division, of the U.S. Department of Energy under Contract No. DE-AC02-05CH11231 to Lawrence Berkeley National Laboratory. The detailed comments from two anonymous reviewers and the suggestions from the Associate Editor, Prof. Sumit Chakraborty, were substantial to the improvement of the manuscript.

References

(1) Palut, J.-M.; Montarnal, Ph.; Gautschi, A.; Tevissen, E.; Mouche, E. Characterisation of HTO Diffusion Properties by an In Situ Tracer Experiment in Opalinus Clay at Mont Terri. J. Contam. Hydrol. 2003, 61, 203−218. (2) Tevissen, E.; Soler, J. M. Mont Terri Project. DI Experiment. Synthesis Report. Mont Terri Project, Technical Report TR 2001−05, Switzerland, 2003. www.mont-terri.ch. (3) Gomez-Herna´ ndez, J. J.; Guardiola-Albert, C.´ Flow Mechanism (FM-C) Experiment: Three Dimensional Model Predictions of Tracer Evolution of HTO and Iodine in the Main Fault. Mont Terri Project, Technical Report 2000−08, Switzerland, 2004. www.mont-terri.ch. (4) Tevissen, E.; Soler, J. M.; Montarnal, P.; Gautschi, A.; Van loon, L. Comparison Between In Situ and Laboratory Diffusion Studies of HTO and Halides in Opalinus Clay from the Mont Terri. Radiochim. Acta 2004, 92, 781−786. (5) Van Loon, L. R.; Wersin, P.; Soler, J. M.; Eikenberg, J.; Gimmi, T.; Hernan, P.; Dewonck, S.; Matray, J.-M. In-Situ Diffusion of HTO,´ 22Na+ , Cs+ and I− in Opalinus Clay at the Mont Terri Underground Rock Laboratory. Radiochim. Acta 2004, 92, 757−763. (6) Wersin, P.; Van Loon, L. R.; Soler, J. M.; Yllera, A.; Eikenberg, J.; Gimmi, T.; Hernan, P.; Boisson, J.-Y. Long-Term Diffusion´

Experiment at Mont Terri: First Results from Field and Laboratory Data. Appl. Clay Sci. 2004, 26, 123−135. (7) Yllera, A.; Hernandez, A.; Mingarro, M.; Quejido, A.; Sedano, L.´ A.; Soler, J. M.; Samper, J.; Molinero, J.; Barcala, J. M.; Martín, P. L.; Fernandez, M.; Wersin, P.; Rivas, P.; Herna´ n, P. DI-B Experiment:´ Planning, Design and Performance of an In Situ Diffusion Experiment in the Opalinus Clay Formation. Appl. Clay Sci. 2004, 26, 181−196. (8) Samper, J.; Yang, C.; Naves, A.; Yllera, A.; Hernandez, A.;´ Molinero, J.; Soler, J. M.; Hernan, P.; Mayor, J. C.; Astudillo, J. A´ Fully 3-D Anisotropic Numerical Model of the DI-B In Situ Diffusion Experiment in the Opalinus Clay Formation. Phys. Chem. Earth 2006, 31, 531−540. (9) Wersin, P.; Baeyens, B.; Bossart, P.; Cartalade, A.; Dewonck, S.; Eikenberg, J.; Fierz, T.; Fisch, H. R.; Gimmi, T.; Grolimund, D.; Hernan, P.; Mo¨ri, A.; Savoye, S.; Soler, J.; van Dorp, F.; Van Loon, L. Long-Term Diffusion Experiment (DI-A): Diffusion of HTO, I−, 22Na+ and Cs+ : Field Activities, Data and Modelling. Mont Terri Project Technical Report 2003−06, Switzerland, 2006. www.mont-terri.ch. (10) Appelo, C. A. J.; Wersin, P. Multicomponent Diffusion Modeling in Clay Systems with Application to the Diffusion of Tritium, Iodide, and Sodium in Opalinus Clay. Environ. Sci. Technol. 2007, 41, 5002−5007. (11) Soler, J. M.; Samper, J.; Yllera, A.; Hernandez, A.; Quejido, A.;´ Fernandez, M.; Yang, C.; Naves, A.; Herna´ n, P.; Wersin, P. The DI-B´ In-Situ Diffusion Experiment at Mont Terri: Results and Modeling. Phys. Chem. Earth 2008, 33, S196−S207. (12) Wersin, P.; Soler, J. M.; Van Loon, L.; Eikenberg, J.; Baeyens, B.; Grolimund, D.; Gimmi, T.; Dewonck, S. Diffusion of HTO, Br−, I −, Cs+ , 85Sr2+ and 60Co2+ in a Clay Formation: Results and Modelling from an In-Situ Experiment in Opalinus Clay. Appl. Geochem. 2008, 23, 678−691. (13) Wersin, P.; Appelo, C. A. J.; Baeyens, B.; Bossart, P.; Dewonck, S.; Eikenberg, J.; Fierz, T.; Fisch, H. R.; Gimmi, T.; Grolimund, D.; Leupin, O. X.; Möri, A.; Soler, J. M.; van Dorp, F.; Van Loon, L. LongTerm Diffusion (DI-A) Experiment: DI-A2: Diffusion of HTO, Br−, I−, Cs+ , 85Sr2+ and 60Co2+: Field Activities, Data and Modelling. Mont Terri Project, Technical Report 2009−04, Switzerland, 2010. www.montterri.ch. (14) Yi, S.; Samper, J.; Naves, A.; Soler, J. M. Identifiability of Diffusion and Retention Parameters of Anionic Tracers from the Diffusion and Retention (DR) experiment. J. Hydrol. 2012, 446−447, 70−76. (15) Yi, S.; Samper, J.; Naves, A.; Soler, J. M. Inverse Estimation of the Effective Diffusion of the Filter in the In Situ Diffusion and Retention (DR) Experiment. Transp. Porous Media 2012, 93, 415− 429. (16) Soler, J. M.; Wersin, P.; Leupin, O. X. Modeling of Cs+ Diffusion and Retention in the DI-A2 Experiment (Mont Terri). Uncertainties in Sorption and Diffusion Parameters. Appl. Geochem. 2013, 33, 191−198. (17) Gimmi, T.; Leupin, O. X.; Eikenberg, J.; Glaus, M. A.; Van Loon, L. R.; Waber, H. N.; Wersin, P.; Wang, H. A. O.; Grolimund, D.; Borca, C. N.; Dewonck, S.; Wittebroodt, C. Anisotropic Diffusion at the Field Scale in a 4-Year Multi-Tracer Diffusion and Retention Experiment - I: Insights from the Experimental Data. Geochim. Cosmochim. Acta 2014, 125, 373−393. (18) Yi, S.; Samper, J.; Naves, A.; Soler, J. M. A Single-Site Reactive Transport Model of Cs+ for the In Situ Diffusion and Retention (DR) Experiment. Environ. Earth Sci. 2015, 74, 3589−3601. (19)

Leupin, O. X.; Van Loon, L. R.; Gimmi, T.; Wersin, P.; Soler, J. M. Exploring Diffusion and Sorption Processes at the Mont Terri Rock Laboratory: Lessons Learned from 20 Years of Field Research. Swiss J. Geosci. 2017, 110, 391−403. (20) Revil, A.; Glover, P. W. J. Nature of Surface Electrical Conductivity in Natural Sands, Sandstones, and Clays. Geophys. Res. Lett. 1998, 25, 691−694. (21) Revil, A. Ionic Diffusivity, Electrical Conductivity, Membrane and Thermoelectric Potentials in Colloids and Granular Porous Media: A Unified Model. J. Colloid Interface Sci. 1999, 212, 503−522. (22) Revil, A.; Jougnot, D. Diffusion of Ions in Unsaturated Porous Materials. J. Colloid Interface Sci. 2008, 319, 226−235. (23) Biesheuvel, P. M.; Fu, Y.; Bazant, M. Z. Electrochemistry and Capacitive Charging of Porous Electrodes in Asymmetric Multicomponent Electrolytes. Russ. J. Electrochem. 2012, 48, 580−592. (24) Suss, M. Size-Based Ion Selectivity of Micropore Electric Double Layers in Capacitive Deionization Electrodes. J. Electrochem. Soc. 2017, 164, E270−E275. (25) Glaus, M. A.; Baeyens, B.; Bradbury, M. H.; Jakob, A.; Van Loon, L. R.; Yaroshchuck, A. Diffusion of Na and Sr in Montmorillonite: Evidence of Interlayer Diffusion Being the Dominant Pathway at High Compaction. Environ. Sci. Technol. 2007, 41, 478−485. (26) Birgersson, M.; Karnland, O. Ion Equilibrium Between Montmorillonite Interlayer Space and an External Solution - Consequences for Diffusional Transport. Geochim. Cosmochim. Acta 2009, 73, 1908−1923. (27) Glaus, M. A.; Frick, S.; Rosse, R.; Van Loon, L. R. Comparative´ Study of Tracer Diffusion of HTO, 22Na+ and 36Cl− in Compacted Kaolinite, Illite and Montmorillonite. Geochim. Cosmochim. Acta 2010, 74, 1999−2010. (28) Glaus, M. A.; Birgersson, M.; Karnland, O.; Van Loon, L. R. Seeming Steady-State Uphill Diffusion of 22Na+ in Compacted Montmorillonite. Environ. Sci. Technol. 2013, 47, 11522−11527. (29) Tertre, E.; Delville, A.; Pret, D.; Hubert, F.; Ferrage, E. (2015) Cation Diffusion in the Interlayer Space of Swelling Clay Minerals - A Combined Macroscopic and Microscopic Study. Geochim. Cosmochim. Acta 2015, 149, 251−267. (30) Birgersson, M. A General Framework for Ion Equilibrium Calculations in Compacted Bentonite. Geochim. Cosmochim. Acta 2017, 200, 186−200. (31) Xiong, Q.; Jivkov, A. P. Anion Diffusion in Clay-Rich Sedimentary Rocks − A Pore Network Modelling. Appl. Clay Sci. 2018, 161, 374−384. (32) Steefel, C. I.; Appelo, C. A. J.; Arora, B.; Jacques, D.; Kalbacher, T.; Kolditz, O.; Lagneau, V.; Lichtner, P. C.; Mayer, K. U.; Meeussen, J. C. L.; Molins, S.; Moulton, D.; Shao, H.; Simunek, J.; Spycher, N.; Yabusaki, S. B.; Yeh, G. T. Reactive Transport Codes for Subsurface Environmental Simulation. Comput. Geosci. 2015, 19, 445−478. (33) Gimmi, T.; Alt-Epping, P. Simulating Donnan Equilibria Based on the Nernst-Planck Equation. Geochim. Cosmochim. Acta 2018, 232, 1−13. (34) Van Loon, L. R.; Soler, J. M. Diffusion of HTO, 36Cl−, 125I − and 22Na+ in Opalinus Clay: Effect of Confining Pressure, Sample Orientation, Sample Depth and Temperature. Nagra Technical Report NTB-03−07, Nagra, Wettingen, Switzerland, 2003. www.nagra.ch. (35) Tournassat, C.; Steefel, C. I. In Pore-Scale Geochemical Processes; Steefel, C. I., Emmanuel, S., Anovitz, L. M., Eds.; Reviews in Mineralogy & Geochemistry; Mineralogical Society of

America: Chantilly, VA, 2015; Vol. 80, pp 287−329. (36) Tournassat, C.; Appelo, C. A. J. Modelling Approaches for Anion-Exclusion in Compacted Na-Bentonite. Geochim. Cosmochim. Acta 2011, 75, 3698−3710. (37) Bradbury, M. H.; Baeyens, B. A Generalised Sorption Model for the Concentration Dependent Uptake of Caesium by Argillaceous Rocks. J. Contam. Hydrol. 2000, 42, 141−163. (38) Van Loon, L. R.; Baeyens, B.; Bradbury, M. H. The Sorption Behaviour of Caesium on Opalinus Clay: A Comparison Between Intact and Crushed Material. Appl. Geochem. 2009, 24, 999−1004. (39) Jakob, A.; Pfingsten, W.; Van Loon, L. Effects of Sorption Competition on Caesium Diffusion Through Compacted Argillaceous Rock. Geochim. Cosmochim. Acta 2009, 73, 2441−2456. (40) Waber, H. N.; Gaucher, E. C.; Fernandez, A. M.; Bath, A. In´ Geochemistry of Water in the Opalinus Clay Formation at the Mont Terri Laboratory; Pearson, F. J.; Arcos, D.; Bath, E.; Boisson, J. Y.; Fernandez, A. M.; Ga´ bler, H.-E.; Gaucher, E.; Gautschi, A.; Grï¨ ffault, L.; Hernan, P.; Waber, H. N. Mont Terri Project, Technical Report´ 2003−03 (Annex), Switzerland, 2002. www.mont-terri.ch. (41) Wolery, T. J.; Jackson, K. J.; Bourcier, W. L.; Bruton, C. J.; Viani, B. E.; Knauss, K. G.; Delany, J. M. In Chemical Modeling of Aqueous Systems II; Melchior, C., Bassett, R. L., Eds.; ACS Symposium Series 416; American Chemical Society: Washington, DC, 1990; pp 104−116. (42) Horseman, S. T.; Higgo, J. J. W.; Alexander, J.; Harrington, J. F. Water, Gas and Solute Movement Through Argillaceous Media. NEA/ OECD Report CC-96/1, Paris, France, 1996. www.oecd-nea.org/rwm/reports/1996/water.pdf. (43) Stumm, W.; Morgan, J. J. Aquatic Chemistry. Chemical Equilibria and Rates in Natural Waters, third ed.; John Wiley & Sons: New York, 1996. (44) Gimmi, T.; Kosakowski, G. How Mobile are Sorbed Cations in Clays and Clay Rocks? Environ. Sci. Technol. 2011, 45, 1443−1449. (45) Baeyens, B.; Bradbury, M. H. A Physico-Chemical Characterisation Technique for Determining the Pore-Water Chemistry in Argillaceous Rocks. Nagra Technical Report 90−40, Nagra, Wettingen, Switzerland, 1991. www.nagra.ch. (46) Baeyens, B.; Bradbury, M. H. Physico-Chemical Characterisation and Calculated In Situ Porewater Chemistries for a Low Permeability Palfris Marl Sample from Wellenberg. Nagra Technical Report 94−22, Nagra, Wettingen, Switzerland, 1994. www.nagra.ch. (47) Pearson, F. J.; Arcos, D.; Bath, E.; Boisson, J. Y.; Fernandez, A.´ M.; Gabler, H.-E.; Gaucher, E.; Gautschi, A.; Grï¨ ffault, L.; Hernan, P.;´ Waber, H. N. Geochemistry of Water in the Opalinus Clay Formation at the Mont Terri Laboratory. Mont Terri Project, Technical Report 2003−03 (Annex), Switzerland, 2002. www.mont-terri.ch.